Supplementary Information

Spatio-spectral 4D Coherent Ranging Using a Flutter-wavelength-swept Laser

Dawoon Jeong[1], Min Uk Jung[1], Hansol Jang[3], Taeho Jeong[4], Hyunsoo Kim[4], Sanghyeok Yang[4], Janghyeon Lee[4], Chang-Seok Kim[1,2,*]

[1]Department of Cogno-Mechatronics Engineering, Pusan National University, 2 Busandaehak-ro 63beon-gil, Busan, 46241, South Korea

[2]Engineering Research Center for Color-Modulated Extra-Sensory Perception Technology, Pusan National University, Busan 46241, Korea

[3]Ground Technology Research Institute, Agency for Defense Development, Daejeon 34186, South Korea

[4]Electronic Devices Research Team, Hyundai Motor Company, 37 Cheoldobangmulgwan-ro, Uiwang-si, Gyeonggi-do, 16082, South Korea

*Corresponding Author: ckim@pusan.ac.kr (Chang-Seok Kim)

Specifications of the FWSL

The flutter-wavelength-swept laser (FWSL) proposed in this study is a wavelength-swept laser for long-range coherent light detection and ranging (LiDAR). Among the major factors required for a laser source for remote sensing, the long coherence length is the most basic. The measurement results of our FWSL for instantaneous linewidth, which is directly related to coherence length, is shown in Supplementary Fig. 1(a). The spectrum measured from the self-heterodyne interferometer is shown, and the half-width at half-maximum (HWHM) of the Lorentzian fitting of the spectrum is 124 kHz. The coherence length corresponding to a linewidth of 124 kHz at the center wavelength of 1560 nm is approximately 770 m[1,2].

Sweep linearity is another important factor required in a laser source for accurate, coherent ranging. Coherent LiDAR systems using commercial wavelength-swept lasers typically require a separate sweep linearization process. However, no linearization process is included in our system because FWSL guarantees high sweep linearity. The sweep linearity has been proven by wavelength modulation results for coherent ranging at a single point in the main text (Fig. 2(e)). First, to measure linearity, two interference signals with a phase difference of 90 ° were obtained from a fiber-based 4 × 4 Mach-Zehnder interferometer. The phase change of the laser source was extracted through I-Q demodulation and converted into the relative wavenumber according to the relation $I_n = A_n \cos(2k\Delta z + \emptyset_n)$ where I_n, A_n, k, Δz, and $\emptyset$ are the interference signal, signal amplitude, wavenumber, optical path difference, and phase, respectively[3,4]. For wavelength modulation during the measurement, the EOPM was driven with a triangular waveform with an amplitude of 200 Vpp and a rate of 100 kHz, while the WS was fixed at a center wavelength of 1535 nm. Supplementary Fig. 1(b) shows one of the raw interference signals measured from the interferometer, while Supplement Fig. 1(c) shows the modulated wavelength. As mentioned in the text, the linearity of the up-chirp and down-chirp was 0.99997 and 0.99987, respectively. The sweep linearity of our FWSL was sufficient for coherent ranging without additional sweep linearization.

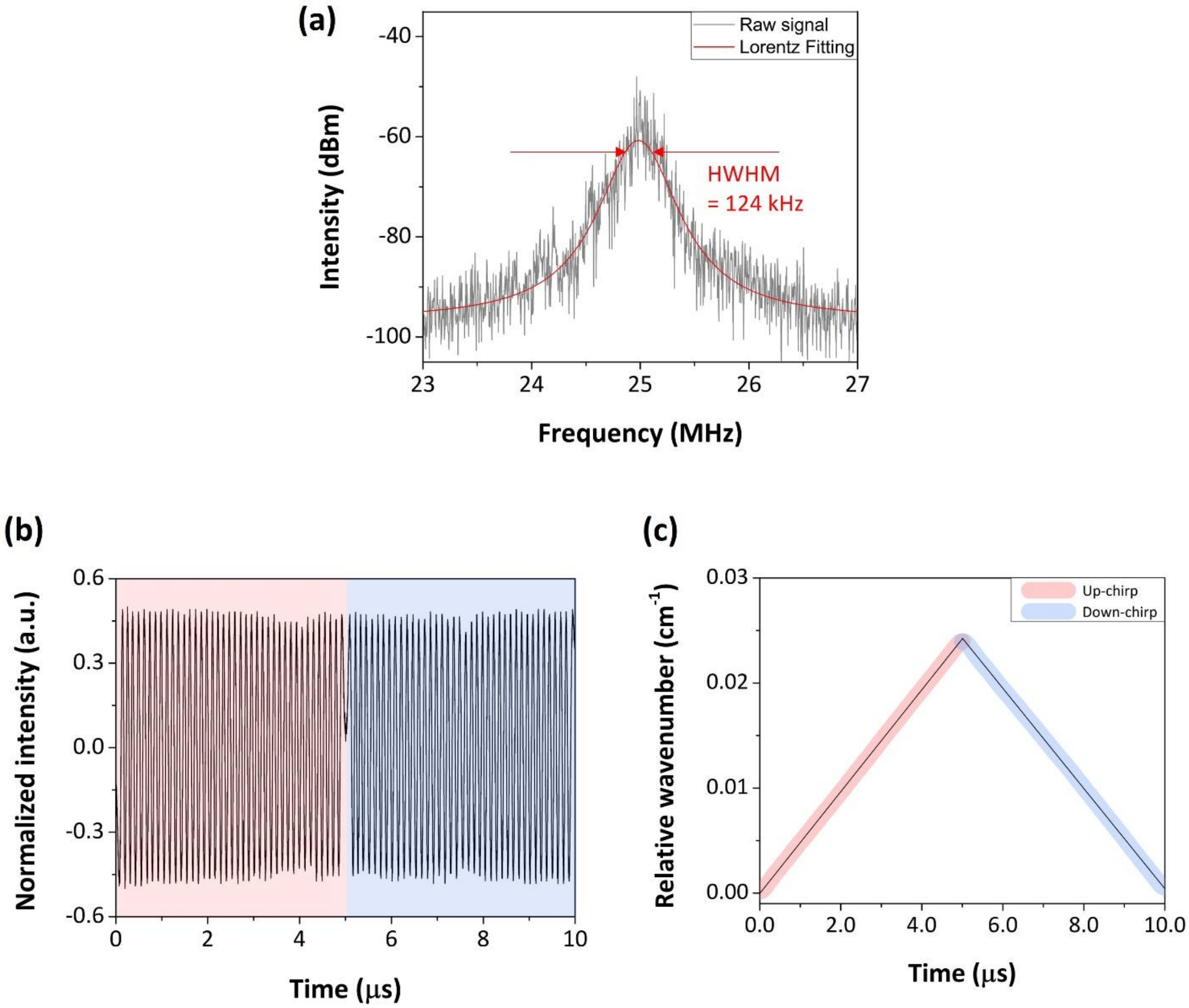

Supplementary Fig. 1 | FWSL specifications. (a) Linewidth measured by the self-heterodyne interferometer; **(b)** Raw interference signal during single wavelength modulation measured from the 4 × 4 Mach-Zehnder interferometer; **(c)** SD of the measurements at the corresponding distances.

Measurement accuracy and precision by FWSL

The one-dimensional (1D) coherent measurement results performed to analyze the accuracy and precision of our LiDAR system using FWSL are shown in Supplementary Fig. 2. The setup for the measurement was the same as the experimental setup described in the main text. The electro-optic phase modulator (EOPM) was modulated under the same conditions as in the experiment, but the measurement was conducted without any lateral scanning. Both AOD and WS were set to the center acoustic frequency and center wavelength and kept fixed. The measurement target was a retroreflective tape, and the distance of the target was measured from 1–25 m at intervals of 2 m. The average distance and error rate of the results measured 1000 times are shown in Supplementary Fig. 2(a). The results show that distances up to 25 m are well measured, with a linearity of 0.9999. Except for the 1 m distance, the measured values have an error rate of less than 10%. Relatively high error values were assumed to occur in regions outside the working distance of the optical system used. Supplementary Fig. 2(b) shows the standard deviation (SD) of 1000 measurement results, showing system precision. The SD tended to increase with the distance to the target, but all the values recorded were below 0.04 m. The results demonstrate that the proposed FWSL enables precise coherent measurements.

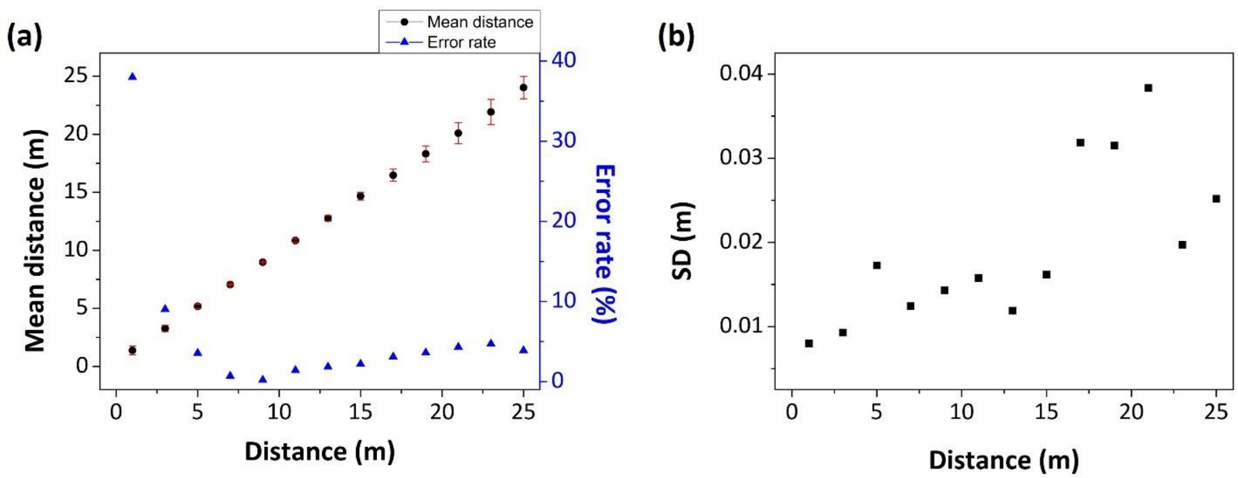

Supplementary Fig. 2 | 1D coherent ranging results. (a) Mean distance measured at different distances with error rate; **(b)** SD of the measurements at the corresponding distances.

Coherent measurement on a rotating disk

The rotating disk used to demonstrate four-dimensional (4D) coherent ranging is shown in Supplementary Fig. 3(a). The retroreflective tape was attached to the disk's surface, whose radius was 0.125 m. The disk was rotated at 770 rpm, and the corresponding tangential velocity was approximately 10 m/s. The rotating disk was located at a distance of 1 m from the transmission grating (TG), and the theoretical velocity along the optical axis according to the horizontal field of view (FOV) is shown in Supplementary Fig. 3(b). Coherent measurement was performed for the region where the linear velocity change was assured. The region of interest (ROI) is depicted as a red box in Supplementary Fig. 3(a), and the corresponding theoretical velocity is shown in Supplementary Fig. 3(b). Supplementary Fig. 3(c) shows the error value of the velocity measurement results in detail.

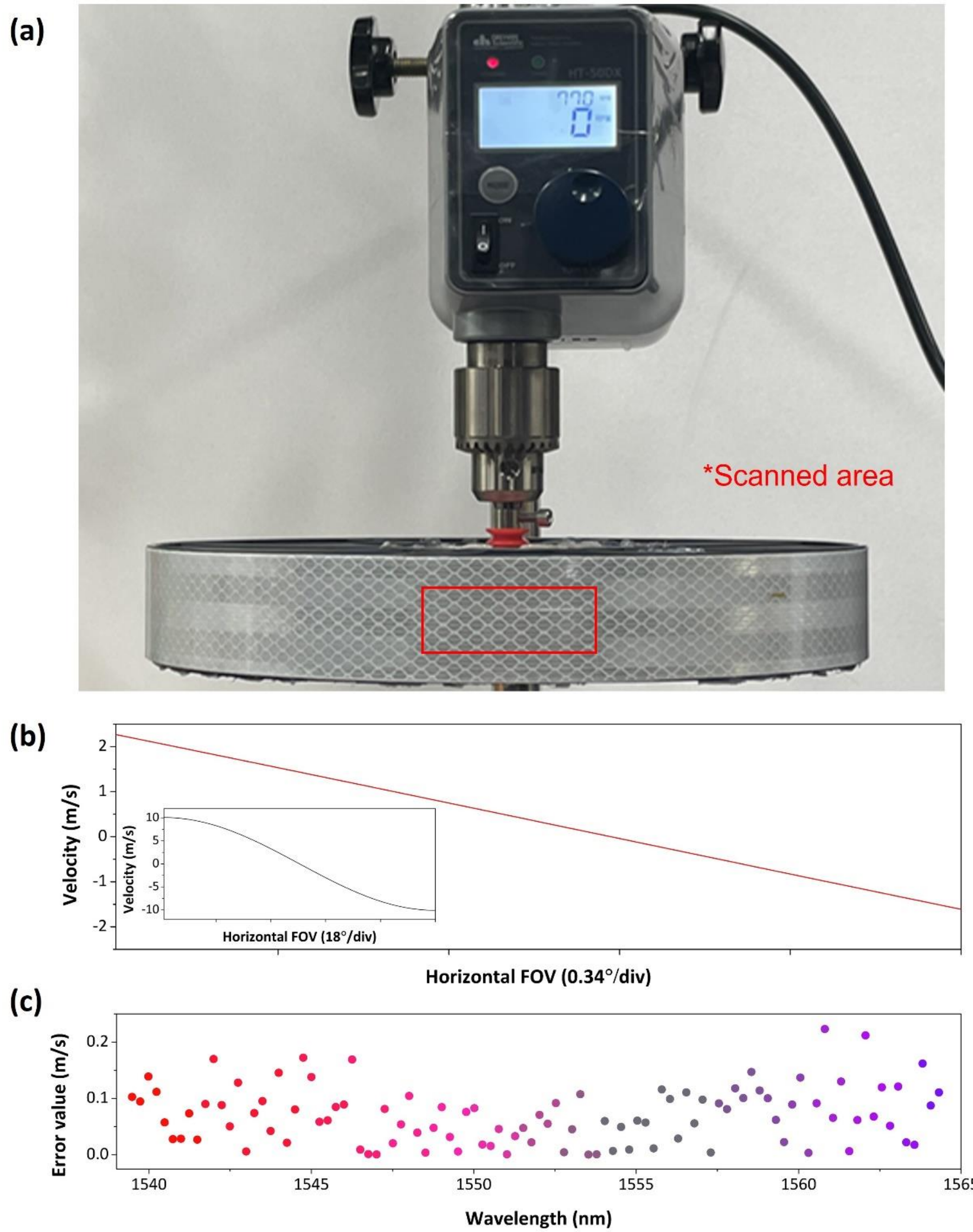

Supplementary Fig. 3: Details of coherent measurement on the rotating disk. (a) Photograph of the rotating disk; **(b)** Theoretical velocity along the optical axis of the rotating disk for the scanned area. The inset is the theoretical velocity for the whole area of the disk; **(c)** Error value of the velocity measurement.

Scenes for 4D coherent ranging

The design of Scene A for room-scale 3D distance imaging is shown in Supplementary Fig. 4(a). The first bus, police car, tunneled bridge, and last white screen are located at 4.8 m, 5.4 m, 6 m, and 7.3 m from the TG, respectively.

The design of Scene B for long-range 3D distance imaging is shown in Supplementary Fig. 4(b). The first box on the far right, second box, third box, fourth box, and last wall are located at 13.5 m, 16 m, 18.5 m, 21 m, and 22.5 m from the TG, respectively.

The design of Scene C for simultaneous 4D distance and velocity imaging is shown in Supplementary Fig. 4(c). The upper part of the tunneled bridge of Scene A is set as the ROI, and the stationary models (two model trees and a traffic light) are located at intervals of 0.3 m from 6 m in the order mentioned.

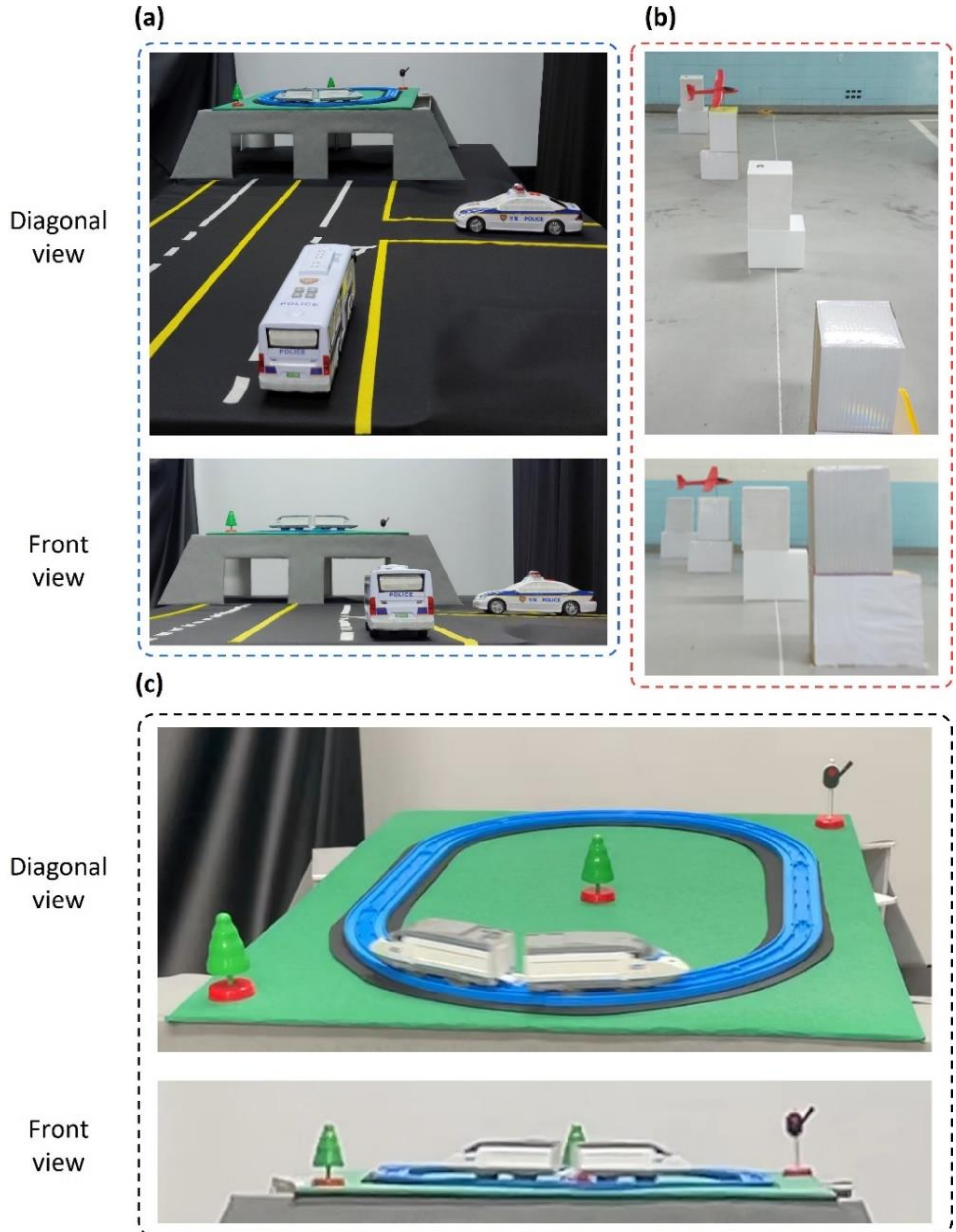

Supplementary Fig. 4: Photographs of the scenarios for 4D coherent ranging of (a) Scene A, (b) Scene B, and (c) Scene C.

Reference

1 Okoshi, T., Kikuchi, K. & Nakayama, A. Novel method for high resolution measurement of laser output spectrum. *Electronics letters* **16**, 630-631 (1980).

2 Mercer, L. B. 1/f frequency noise effects on self-heterodyne linewidth measurements. *J. Lightwave Technol.* **9**, 485-493 (1991).

3 Park, S., Rim, S., Kim, Y. & Lee, B. H. Noncontact photoacoustic imaging based on optical quadrature detection with a multiport interferometer. *Optics letters* **44**, 2590-2593 (2019).

4 Choma, M. A., Yang, C. & Izatt, J. A. Instantaneous quadrature low-coherence interferometry with 3× 3 fiber-optic couplers. *Optics letters* **28**, 2162-2164 (2003).